Spectroscopic diagnostics for the plasma edge of RFX-mod2 device

M. Agostini[1,2], M. La Matina[1,3], M. Ugoletti[1,2], E.Girotto[1], M.Magagna[1], L.Carraro[1,2], M.Zuin[1,2]

[1] *Consorzio RFX, Padova, Italy*

[2] *Istituto per la Scienza e la Tecnologia dei Plasmi, CNR, Padova, Italy*

[3] *Centro Ricerche Fusione – University of Padova, Italy*

RFX-mod2 experiment is the upgraded version of RFX-mod Reversed Field Pinch device, designed to obtain improvements in the magnetic boundary [1]. In order to characterize the edge region of the plasma, different spectroscopic diagnostics in the visible range have been designed to study a large part of the internal wall. The 3D plasma-wall interaction will be monitored by 7 visible cameras equipped with C I filters; a MANTIS [2] device integrates this information by measuring different emission lines; the Light Impurity Tomography (LIT) will provide the poloidal structure of the plasma edge by measuring 3 different ion species; a Thermal Helium Beam will measure n_e and T_e profiles in the edge, and the Gas Puff Imaging the high frequency turbulence [3]. All together, they would allow a complete characterization of the 3D plasma edge, and of the interaction between magnetic topology, plasma shape, and turbulent transport.

This paper describes the optical setup of the LIT diagnostic, and characterizes its performances. The diagnostic consists of 7 cameras, installed in 7 different portholes around the poloidal direction at a fixed toroidal angle, with changeable interferential filters (H_α at 656nm, He I at 668nm, and C III at 465nm). The 7 cameras observe line-integrated signals, and the 2D map of the emissivity of the specific ion species selected by the interferential filter is obtained with a tomographic inversion. The global layout and the optical setup of a single camera are shown in Figure 1. Each camera has a series of 3 objectives: a first lens with f=24mm collects the light from the plasma; a f=85 mm lens collimates the light beam, ensuring it impinges perpendicularly on the filter; a third f=85mm lens focuses the image on the camera. For having more fans and increasing the spatial resolution, one or two mirrors can be installed in vacuum in front of the first objective. The resulting line of sights (LoSs) are outlined in the left panel of Figure 1. The total fans obtained are 13, whose centres are the black dots in the same figure. The selected camera is a USB3 Basler acA1920-155um, with square pixels with size 5.86 μm, and a sensor of 11.3x7.1 mm^2. With this optical setup, each camera observes a region at 0.5 m of about 220x140 mm^2. The maximum framerate is 165 Hz at 8 bit and 100 Hz at 12 bit; in this way it is possible to follow the time evolution of the plasma wall interaction and the deformation of the plasma due to the rotation of the magnetic modes. Four NVIDIA Jetson Orin will control the acquisition

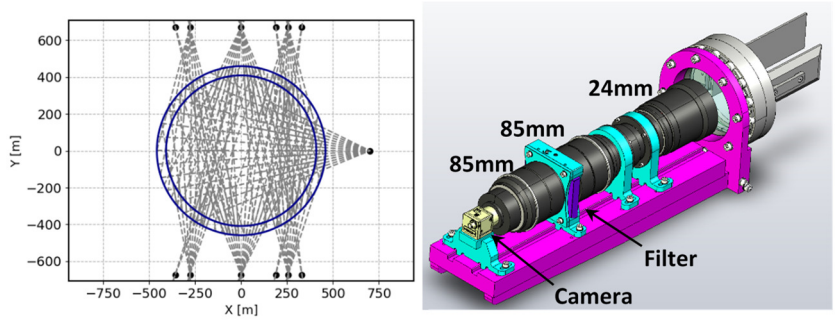

Figure 1: poloidal section of RFX-mod2 with the layout of the 7 cameras and lines of sight (left); sketch of the optical setup of the single camera (right).

of two cameras each, and can provide also real time analysis of the collected images.

In order to characterize the spatial resolution of the diagnostic, different simulations of the plasma edge emission of ions ε_{simu} have been performed, resulting from a superposition of m=0,1,2 modes. Along the radial direction, the emissivity shell is simulated with a semi-Gaussian shape function, with its maximum at the wall, and with a radial width σ. ε_{simu} is integrated numerically along the different LoSs to obtain the expected experimental signals. The tomographic algorithm developed is based on the pixels method: the poloidal region is divided into 50 pixels, with a radial dimension Δr, and constant emissivity. The emissivity of each pixels ε_i^k at iteration *k* is obtained by using the ML-EM iterative algorithm [4], according the formula:

$$\epsilon_i^{k+1} = \frac{\epsilon_i^k}{\sum_{j=1}^{nlos} a_{i,j}} \cdot \sum_{j=1}^{nlos} \frac{I_j}{\sum_{i=1}^{npix} \epsilon_i^k \, a_{i,j}} a_{i,j}$$

where a_{ik} is the length of the LoS *j* inside the pixel *i*, I_j is the integrated signal of the LoS *j*, *nlos* is the number of LoSs and *npix* the number of pixels. For each emissivity simulated, inversions with different radial size of the pixels are performed; the best pixels size is the one that minimizes the difference between the simulated and inverted integrated signals. In this way we can recover an average radial resolution. Figure 2 shows the poloidal emissivity map: simulation on the left side, and its tomographic reconstruction on the right. The reconstruction well reproduces the simulation, with a minimum emissivity at about θ=45°, and a large maximum at about θ=180°. By varying the radial width of the emission shell (σ) in different simulations, a linear relation between σ and the pixel dimension Δr is recovered. This demonstrates that a coarse radial resolution of the emission shell is attainable, albeit constrained by the limited angular range of the LoSs. The poloidal resolution of 50 pixels (7.2°) is a compromise between a good angular resolution and a good tomographic inversion, and it is sufficient to detect the poloidal variation of the edge plasma emissivity, in presence of m=0,1,2 magnetic modes. The developed technique must be robust enough to provide reliable emissivity inversion, even in presence of noise in the camera signals and uncertainties in the relative calibration of the cameras. To test the first effect, a random uniform noise is added to the integrated signals and then the inversion is performed. The results are shown on the left panel of Figure 3: the black line is the poloidal profile of ε_{simu} (the same simulation of Figure 2), and the red, blue and green lines are the tomographic inversion with different noise levels, as reported in the legend. The effect of the noise is to add a fluctuating component in the emissivity, without compromising the overall result.

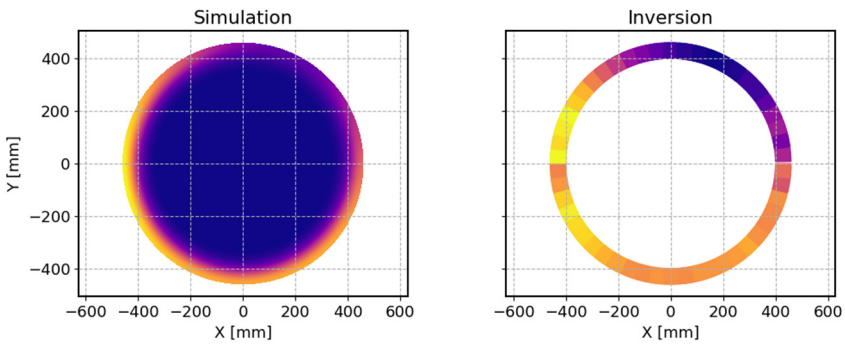

Figure 2: simulated emissivity (left) and its tomographic reconstruction (right).

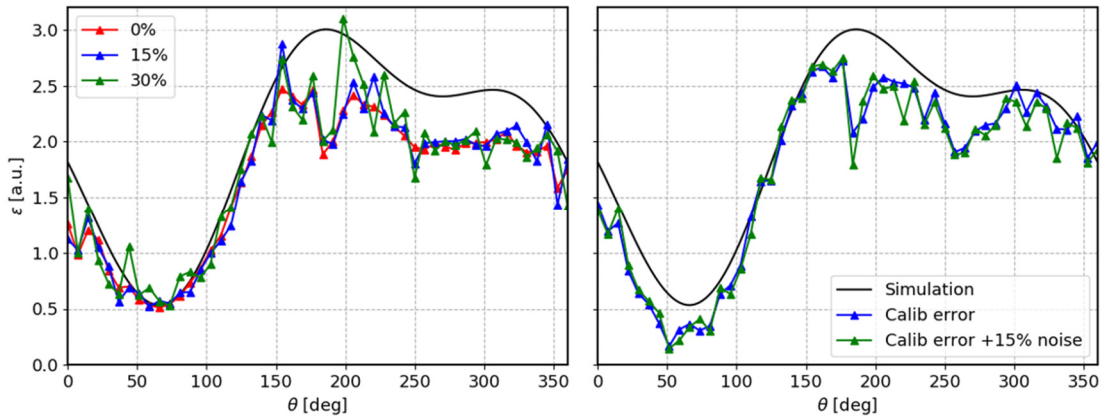

Figure 3: poloidal emissivity profile. Left: simulation in black and tomographic inversion with different noise level in colors. Right: simulation in black and tomographic inversion, with calibration error (blue) and with calibration error + 15% noise.

The effect in the tomographic inversion of the calibration errors of the 7 cameras and of the reflectivity of the different mirrors is studied on the right panel Figure 3. Each optical setup (mirrors, lenses, filter and camera) will be calibrated with a calibrated lamp, and +/-20% level of uncertainty is assumed. To simulate this effect, the integrated signal of the group of LoSs associated with each of the 13 fans is multiplied by a random factor between 0.8 and 1.2, then the tomographic inversion is performed. The right panel of Figure 3 compares ε_{simu} in black, the inversion with the calibration errors in blue, and the inversion with the calibration errors plus 15% random noise in green. The effect of the calibration is larger with respect to the noise. In fact, by affecting a contiguous group of LoSs, it slightly modifies the overall shape of the emissivity profile (around θ=50° in this simulation). The reconstruction still remains reliable, demonstrating that the proposed method can be applied.

Figure 3 shows that the inversion is less reliable on the inner side of the torus (θ=180°), where the reconstructed emissivity shows a systematic decrease. This is due to the poor coverage with LoSs of the inner wall: due to the port limitations, only few of them reach that region, with limited incident angles.

The analysis described shows that the diagnostic setup and the tomographic algorithm developed can invert the simulated emissivity of the edge plasma, also in presence of noise and calibration uncertainties.

Being m=0 and m=1 the largest magnetic poloidal modes in a RFP device [5][6], with similar deformation of the plasma wall interaction, LIT have to be able to distinguish the two different topologies. Simulations (adding a random noise of 15%) with different ratio between m=0 and m=1 modes (A_0/A_1) amplitudes are inverted with the described method, and the resulting emissivities are reported on the left panel of Figure 4. The blue line refers to m=0 mode only, the other colours refer to the different ratio A_0/A_1 reported in the legend.

The inverted emissivity shows different shapes, with a clear increase of the m=1 modulation, moving from blue to black. It is possible to identify in a clearer way the mode structure of the inverted emissivity by applying a spatial Fourier Transform and by measuring the amplitude of the resulting poloidal modes. This is carried out on the right panel of Figure 4, where we compare the modes decomposition of two simulations with different ratio of m=0 and m=1 modes: A_0/A_1=1.1 in black, and A_0/A_1=4 in red. In both the inversions,

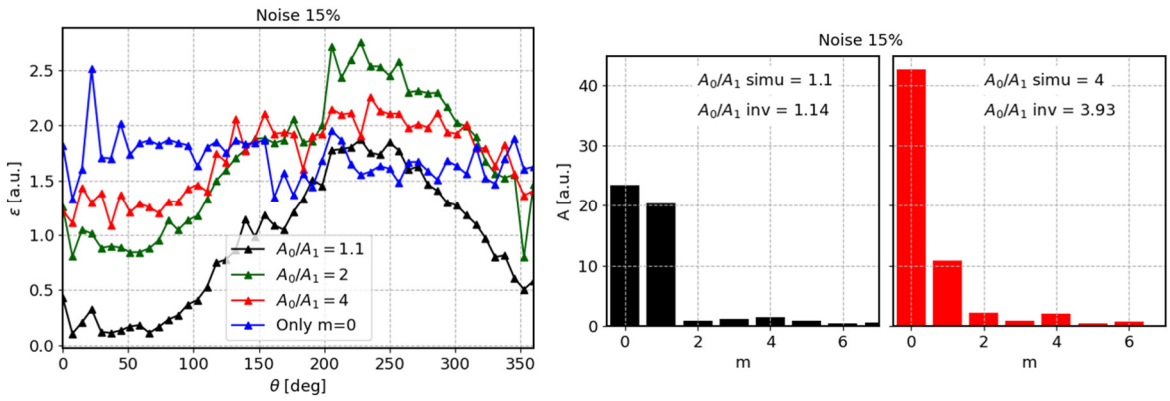

Figure 4: Left: inversion of simulations with different ratios between m=0 and m=1 modes amplitude. Right: poloidal mode numbers of two reconstructions, with same amplitude of m=0 and m=1 modes (black bars) and wit m=0 amplitude 4 time m=1 (red bars). All the simulations with 15% noise added.

higher m components appear in the spectrum, with very small amplitude respect to the 0/1 modes, due to artefacts in the inversions. The important result is that the Fourier transform of the inverted emissivity correctly identifies the relative amplitude of the dominant poloidal modes: by simulating $A_0/A_1 = 1.1$ (black bars) we obtain 1.14, and by simulating $A_0/A_1 = 4$ (red bars) we obtain 3.9. Thus, even if small scale oscillations are present (detected as m>1 components) and even if the reconstruction shows a systematic decrease of the emissivity at $\theta \approx 180°$ due to the not optimal coverage of that region with the LoSs, the poloidal structure of the simulated emissivity is recovered. This result is fundamental, since one of the aim of the diagnostic is to study how the poloidal structure of the edge plasma varies by varying the main plasma parameters such as the electron density, and how it is linked to the poloidal structure of the magnetic deformation [7].

The simulations discussed in the paper show that the LIT diagnostic is capable of characterizing the spatial structure of the emissivity of neutral atoms and low-ionized species at the edge of RFX-mod2. It will be completed and installed in the machine, ready for the first measurements foreseen in 2026.

Acknowledgments

This work has been carried out within the framework of Italian National Recovery and Resilience Plan (NRRP), funded by the European Union—NextGenerationEU (CUP B53C22003070006, 'NEFERTARI'). Views and opinions expressed are however those of the author(s) only and do not necessarily reflect those of the European Union or the European Commission. Neither the European Union nor the European Commission can be held responsible for them.

References

[1] D. Terranova et al. Nucl. Fusion **64** (2024) 076003

[2] A.Perek et al. Rev. Sci. Instrum. **90** (2019) 123514

[3] L.Carraro et al. Nucl. Fusion **64** (2024) 076032

[4] L.A.Shepp and Y.Vardi, IEEE Trans. Med. Imaging **1** (1982) 113

[5] P. Scarin et al. Nucl. Fusion **59** (2019) 086008

[6] P.Porcu et al. Phys. Plasmas **31** (2024) 082506

[7] M.Agostini et al. Nucl. Fusion **57** (2017) 076033